energies

MDPI

Article

Power Reserve from Photovoltaics for Improving Frequency Response in the Isolated System

Olga Poliak [1,2] and Doron Shmilovitz [1,*]

[1] School of Electrical Engineering, Tel Aviv University, Tel Aviv 6997801, Israel
[2] Noga ISO, Fliman 8, Haifa 3508418, Israel
* Correspondence: shmilo@tauex.tau.ac.il

Abstract: Appropriate frequency response is an issue of great importance in power system management, especially in an islanded one. An energy-based method for assessing a system's response, which is needed to prevent under frequency load shedding (UFLS), is introduced. Renewable generation, such as wind turbine (WT) and photovoltaic (PV) facilities, reduces the ability of the power system to resist power imbalances and increases the risks of consumer disconnections by UFLS system, and even of total collapse. To estimate the amount of additional fast power reserve, an equation was developed, relating the moment of inertia, the system demand dynamics, and the available response of synchronous generating units. Clustering units based on their ability to respond to frequency changes in low inertia conditions allows the potential synchronous response to be assessed, providing information of its deficiency in a defined system state. The proposed method was applied to the Israeli power system and up to 307 MW response needed from PV facilities was found for the 350 MW contingency, when the percentage of renewable energy reached 30% of the annual energy production. This study focused on proportional frequency response (PFR) and step frequency response (SFR) that PV facilities can provide. Using this method may contribute to the adoption of PV facilities into the power system without a detrimental impact on frequency response and may even improve the reliability of electricity supply.

Keywords: frequency response; power system; frequency nadir; photovoltaic plants

Citation: Poliak, O.; Shmilovitz, D. Power Reserve from Photovoltaics for Improving Frequency Response in the Isolated System. *Energies* **2023**, *16*, 3595. https://doi.org/10.3390/en16083595

Academic Editor: Paulo Jose Da Costa Branco

Received: 6 March 2023
Revised: 11 April 2023
Accepted: 18 April 2023
Published: 21 April 2023

1. Introduction

Events of forced outage are relatively common and the ability of a power system to overcome this type of contingency is a major requirement. In a power system based on rotating generators, this sudden imbalance between the power consumed by the load and the power produced by power plants will cause a decrease in frequency. The primary response of the generating units to the frequency deviation will slow the frequency decline and eventually stabilize it. In conventional power units, this response is realized by increasing mechanical power, by adding more steam or gas to the turbines [1,2]. If a system's response is not sufficient, a load shedding mechanism disconnects consumers to achieve a balance between production and load. The role of the under frequency load-shedding (UFLS) system is, then, vital in avoiding the deterioration of the frequency and preventing total system collapse. However, disconnecting consumers is undesirable. Therefore, an effective frequency response has a major impact on the reliability of supply. One of the basic criteria for evaluating the security of a power system is the system's frequency response to the trip of the largest generation unit.

In order to prevent UFLS activation, it is necessary to keep the frequency deviation above a certain threshold, which is defined in accordance with the first step of the UFLS system. This goal can be achieved if the sum of primary responses of all generation units in the system together with load relief due to frequency drop is equal to or greater than the power of the tripped unit. The power injection must be carried out within a limited time,

which depends, among other things, on the level of system inertia. In the methods section, we detail the estimation of this time frame and what maximum response can be expected from synchronous generating units within this time.

For an isolated power system such as the one in Israel, an adequate frequency response and proper planning of reserves play a key role. Presently, tens of forced outages of generating units per year cause a significant frequency drop and instigate the use of UFLS, a phenomenon that rarely occurs in large, interconnected systems. Studies conducted on isolated [3,4] as well as interconnected systems [5–7] showed that large-scale integration of renewable energy sources (RES), without inertia and without primary frequency response, weaken the ability of a power system to resist generation trips.

There are many ways [8,9] to prevent degradation in a system's ability to resist the imbalances between production and consumption by devices with fast response, such as batteries, supercapacitors, flywheels, demand side response, etc. However, one of the interesting ways to achieve this goal is to use the renewable facilities themselves, by reserving power and participating in primary frequency control. This has the advantage that no construction of additional facilities is needed. With the help of reserve, PV facilities are able to regulate frequency in both directions: by increasing power on frequency drops and decreasing power on frequency rises, such as synchronous generators, can only do it better. Without mechanical movement, they are able to provide a much faster response and, thereby, cause a more significant effect. Although using the renewable facilities for reserve power was used in recent papers [9–12], not enough attention was given to reserve distribution between generators, which plays a key role in system response.

The most commonly used method to determinate the system frequency's behavior is dynamic simulation of the contingency process. Multiple studies used dynamic simulation, either by checking the system response in one specific condition [9,10,13], or by including it in the optimal unit commitment program in order to determine all possible states of the system during the year [7,11,12,14,15]. For example, it was reported on over one million dynamic simulations for the Australian power system in 2040 [12]. Unit commitment procedure with dynamic frequency stability simulations for different non-synchronous annual penetration levels from 10% to 90% was examined. The frequency stability was investigated for each simulation, without effort to improve it, if the limit was violated. The study [9] examined the integration of RES in Israeli power system in the worst case scenario of year 2025. The frequency behavior following the loss of a large generator was analyzed, with share of RES from 13% to 20% of annual energy. With step-by-step simulation process, it was found that up to 190 MW of storage is required to maintain frequency stability. One of the main conclusions is that locating energy storage systems in the south and distributed PV facilities in the north produce a more balanced system and has a positive impact on frequency nadir.

While simulations are valuable, this methodology has several limitations: (1) it requires dedicated software; (2) it is time-consuming; (3) its results are relevant mostly to the specific system under discussion; (4) it covers a limited time range (usually, a single year); and (5) any change in the model parameters requires repeating the simulation from scratch.

A different approach involves using an equivalent model for the power system with a closed-form solution [16,17] assumes an equal distribution of the reserve between all generators and their uniform response. This assumption is unjustified, as will be shown later. A number of studies in this area were focused on steady-state value of frequency [18–20], which is not sufficient for preventing UFLS.

Thus, there remains a need for an efficient and fast method that can answer two important questions: when it is necessary to keep reserve power in renewable generation plants, and how much reserve is required.

This research presents the analysis of factors that affect frequency response and develops a method to determine the level and time of power injection required to prevent UFLS. The results of this analysis provide a basis for estimating the RES penetration level that can be accepted without a decline in the reliability of supply. Importantly, we propose

a novel equation for evaluating the amount of reserve from PV sources, where we focus on the proportional frequency response (PFR) and step frequency response (SFR) that PV facility can provide.

During the last few years, the FERC (Federal Energy Regulatory Commission) in the United States [21] and ENTSO-E in Europe [22] changed the interconnection agreement so that primary frequency response is required from all facilities, including RES. Advanced requirements for active power control of RES facilities were developed in South Africa and Romania [23], in the Grid Codes of Ireland [24] and in the National Grid, United Kingdom [25]. In Israel, primary frequency response is required for new PV facilities connected to the transmission system [26]. Demonstration projects of utility scale PV plants [27–29] validate their ability for frequency and voltage grid support according to the requirements of system operators.

Using the research results will enable the integration of PV facilities in the power system without negative impact on frequency response and may even improve the reliability of electricity supply to consumers.

This paper is organized as follows: Section 2 presents the methodology we used to calculate the required response power from PV facilities. Section 3 shows how this method may be implemented in case studies of the Israeli power system. The discussion and conclusions are presented in Section 4.

2. Methods

2.1. Frequency Response of the Power System

Testing the system frequency response following loss of the largest generator is a standard procedure for assessing the dynamic stability of the power system. For reliable supply of electricity for consumers, the frequency response is considered satisfactory if it maintains frequency above the level of the first step of the UFLS system.

The frequency behavior during contingencies may be defined by the well-known swing equation, as presented in [1] or [2]. Acceleration power P_{ACC} is defined as the rate of change of kinetic energy, where E_k is the kinetic energy of a turbogenerator with moment of inertia J, rotating with angular velocity ω_M. P_M is the mechanical power at the turbine rotor, and P_E is the generator's electrical load including losses.

$$P_{ACC} = P_M - P_E = \frac{dE_K}{dt} = J\omega_M \frac{d\omega_M}{dt}. \quad (1)$$

For the whole system (1) can be specified by summarizing all the generating units and converting the mechanical velocity ω_M to frequency f with reference to the center of inertia [30]:

$$P_{ACC_{SYS}} = P_{M_{SYS}} - P_{LOAD} = J_{SYS} 4\pi^2 f \frac{df}{dt}. \quad (2)$$

J_{SYS} is the moment of inertia of whole system, including all generating units and rotating loads:

$$J_{SYS} = \sum_{i=1}^{N} \frac{J_i}{p_i^2} + J_{LOAD} \quad (3)$$

where N is the number of generating units, p_i is the number of pole pairs of unit i, J_{LOAD}—moment of inertia of rotating loads, e.g., motors.

In the steady state, the frequency is constant. Hence, the equation $df/dt = 0$ holds, meaning that there is a balance between the mechanical power (generated by turbines) and the electrical power (consumed by load): $P_{MSYS} = P_{LOAD}$. Immediately after a generator trip, the load is distributed among a smaller number of generators. Every synchronized generator increases the active power that it transmits to the grid by decreasing its rotation speed and kinetic energy, providing inertial response. The inertial response of a turbogenerator is immediate and depends on the derivative of the frequency and its moment of inertia, independent of the loading level.

The prime turbine-governor control system of a generation unit adjusts the mechanical power produced by the turbine according to frequency deviations in the system. This additional active power depends on the frequency deviation and the control system parameters and is only possible if there is a power reserve. The timing of the primary frequency response varies between units and can range from several seconds to dozens of seconds.

An additional factor that affects the frequency behavior during a transient is the load-frequency sensitivity. Each load has its own frequency dependence characteristic, but for systemic analysis, it is common practice to use coefficient D, which is measured in units $\frac{\%MW}{\%Hz}$, to calculate the *Load Relief* [30,31] for frequency deviation Δf and initial load power P_{LOAD}:

$$Load\ Relief = D * P_{LOAD} * \frac{\Delta f}{f_{nom}}. \tag{4}$$

The frequency's behavior after a contingency is a result of multiple interdependent processes, and simulations are conducted to find the frequency nadir. In this study, we offered an alternative for computing the frequency's behavior, by setting a minimal point in advance, such that load shedding was avoided. For example, in the Israeli system, the first step of load shedding is activated at 49.4 Hz. Therefore, we chose the minimal frequency point of 49.45 Hz, which left a margin until the point of load shedding was activated, considering different initial values of frequency before the contingency.

The frequency of the system will stay above the set threshold as long as the additional mechanical power from all production units within the specified time frame will be equal to or larger than the magnitude of the contingency minus *Load Relief*. To estimate the time frame until the frequency nadir, the initial *ROCOF* (Rate of Change of Frequency) will be used. The initial $ROCOF_0$ can be easily computed using (2), where ΔP is the size of the contingency, and J_{FO} is the moment of inertia of a tripped unit.

$$ROCOF_0 = \left.\frac{df}{dt}\right|_{t=0} = -\frac{\Delta P}{(J_{SYS} - J_{FO})4\pi^2 f_0} \tag{5}$$

If the power of the load and the generator does not change, the acceleration power will remain constant. Therefore, the decrease in the frequency will be almost linear (within the set frequency range) and will reach the frequency threshold within time t_1, as shown in Figure 1.

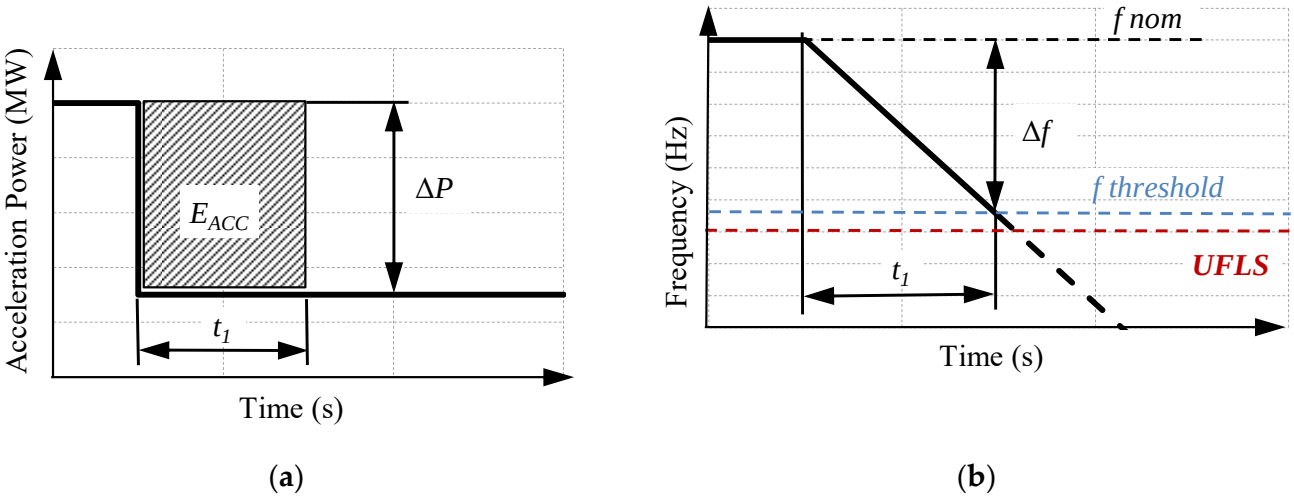

Figure 1. (**a**) Fixed acceleration power; (**b**) linear frequency deviation.

Assuming linear change in the acceleration power, the frequency will decrease following a quadratic function, requiring twice the time of t_1 to reach the minimal point, as

shown in Figure 2. This results in the following time estimate until the frequency nadir is reached t_{FN}:

$$t_{FN} = 2\frac{\Delta f}{ROCOF_0} = \frac{\Delta f * (J_{SYS} - J_{FO})8\pi^2 f_0}{\Delta P}. \quad (6)$$

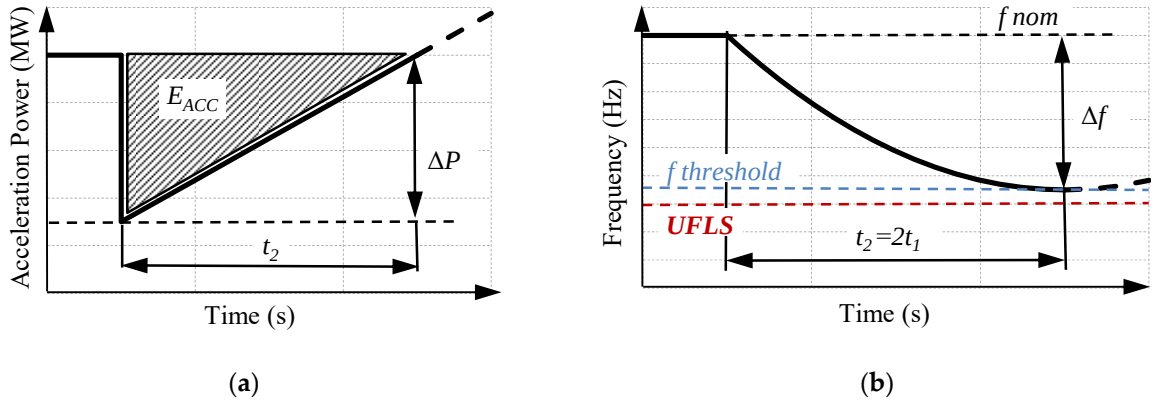

(**a**) (**b**)

Figure 2. (**a**) Linear change in acceleration power; (**b**) quadratic frequency deviation.

2.2. Primary Frequency Response of Synchronous Units

The proposal in Section 2.1 will be tested using the Israeli power system as a case study. We chose typical unit commitment configurations for synchronous production only for three different system demand levels: low (6 GW), medium (9 GW), and high (11 GW). There is a strong correlation between the system load and its inertia: the higher the system demand is, the more production units are on-line, resulting in higher system moment of inertia. The reserve allocation between the units was defined such that a 350 MW generation trip will result in arresting the frequency at the 49.45 Hz threshold, preventing load shedding. The system acceleration power and the frequency's behavior are shown in Figure 3. The black dots mark the points of frequency nadir for each of the three inertia conditions. The times until the frequency nadir was reached in the three inertia conditions were both simulated and calculated using (6) (see Table 1).

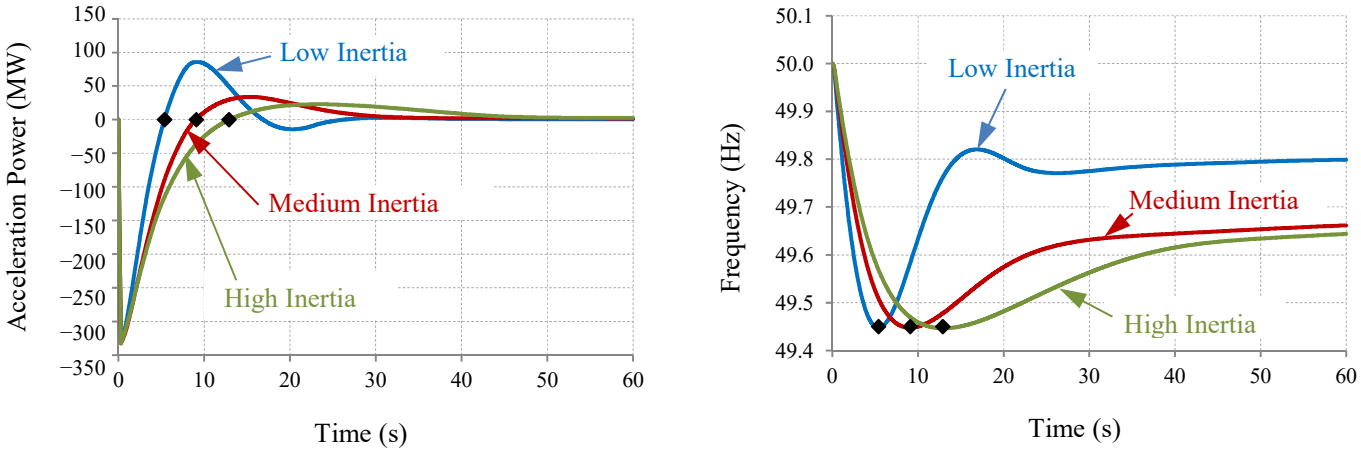

(**a**) (**b**)

Figure 3. (**a**) Acceleration power; (**b**) frequency; in the Israeli power system after 350 MW generation trip, different inertia conditions.

Table 1. Time until Frequency Nadir for Different Inertia Conditions.

Inertia Condition	System Moment of Inertia, J_{SYS}	Calculated t_{FN}	Simulated t_{FN}
	$\times 10^6$ kg·m^2	s	s
Low	0.86	5.02	5.38
Medium	1.16	6.86	9.03
High	1.37	8.18	12.95

The same trend emerges from the times computed via simulation and via calculation (6). Specifically, the higher the system inertia, the slower was the frequency drop. In cases of medium and high inertia, the linear computation resulted in overly conservative estimates. As shown in Figure 3a, the acceleration power until point of minimal frequency was noticeably not linear in the medium and high inertia cases. However, for the low inertia condition, when the time of *FN* is much smaller than response time of the governor [2,32], linear approximation works well. With the high penetration of RES, the system inertia is expected to decrease, justifying the use of (6).

On the other hand, the time of *FN* should not be too small. For the range of our interest it fits well: if initial $ROCOF_0$ limited by 0.5 Hz/s [12], so time of *FN* (for Δf = 0.55 Hz) will be equal to or greater than 2.2 s. This time-window gave good results, which was tested and proved by simulation.

The responses of different generation units in the three inertia conditions above were tested as a function of the reserve. Steam units of Type 1 (Figure 4) had a control system that is limited by environmental considerations. In these units, the additional mechanical power within the first several seconds was negligible. So, for low inertia condition, it may be defined as zero-response contribution group.

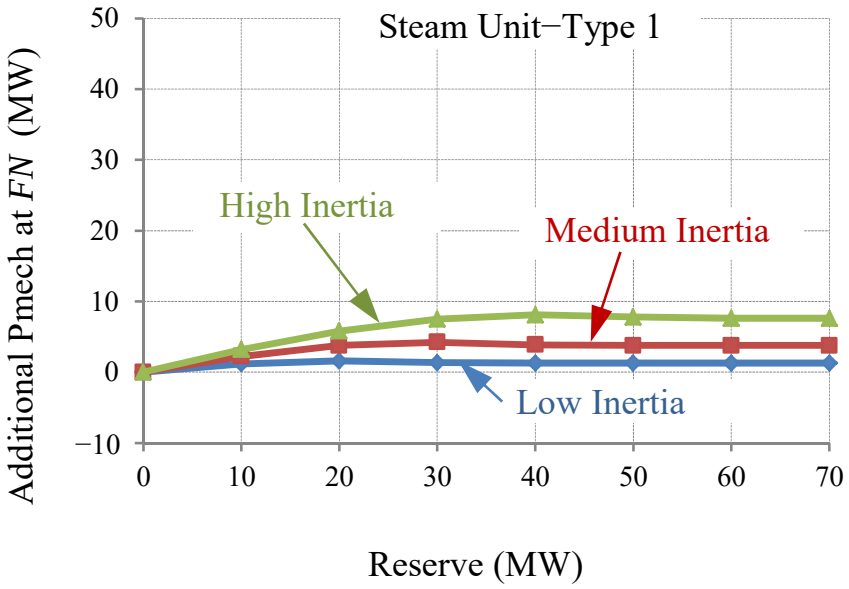

Figure 4. Additional mechanical power of Steam Unit—Type 1 as response for 350 MW trip, in 3 inertia conditions.

Steam units of Type 2 (Figure 5) had a fast control system and could produce up to 35 MW of additional mechanical power, independent of inertia. This group of units may be defined as fixed size response group.

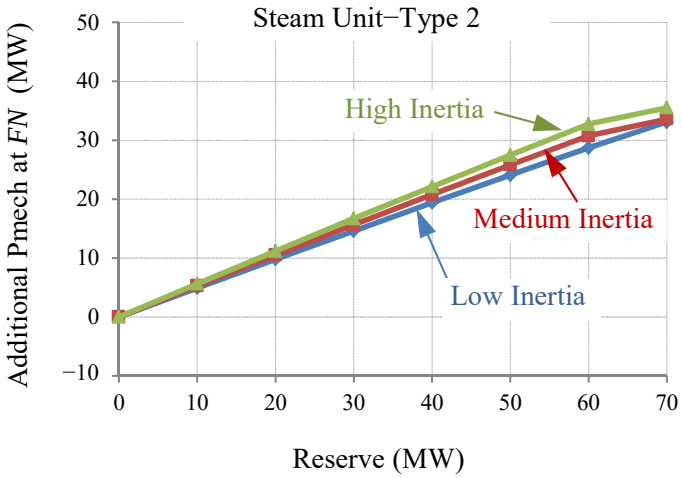

Figure 5. Additional mechanical power of Steam Unit—Type 2 as response for 350 MW trip, in 3 inertia conditions.

In combined cycle (CC) units, the availability of additional mechanical power is strongly dependent on the time until the frequency nadir (Figure 6). For example, in the case of low system inertia, if the combined cycle unit has over 50 MW in reserve, it is possible to add only 17 MW until the frequency nadir is reached. Naturally, different combined cycle units differ slightly in their characteristics, but for the purposes of this study, we set a constant rate of α_{CC} = 3.5 MW/s during the first seconds. Third group's contribution to the system response may be defined as time-dependent power injection, concerning the time of frequency nadir.

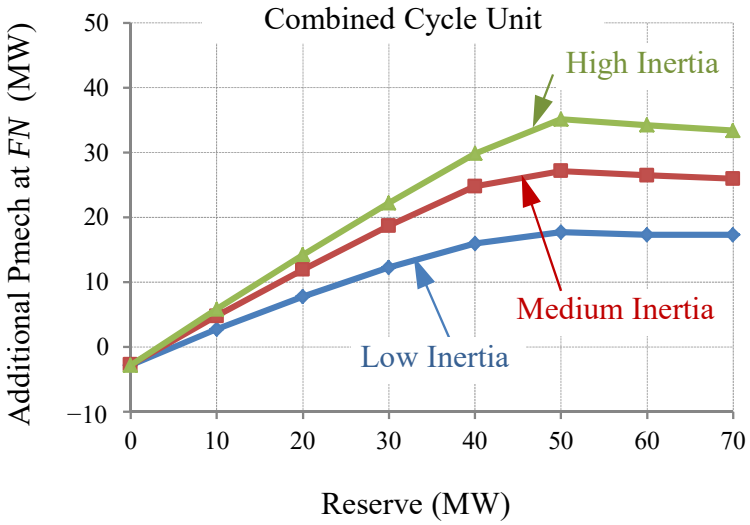

Figure 6. Additional mechanical power of Combined Cycle Unit as response for 350 MW trip, in 3 inertia conditions.

How many synchronous units can be connected to the system at any given time can be determined using the residual load, defined as load demand minus renewable power output. If the residual load allows committing of n steam units with fixed size response ($Response_{SU2}$) and m combined cycle units with a time-dependent response, it is possible to estimate the available response of synchronous units ($Response_{SG}$) using the following method:

$$Response_{SG} = n * Response_{SU2} + (m-1) * \alpha_{CC} * t_{FN} \quad (7)$$

We chose to trip combined cycle unit, so the response of combined cycle units in (7) is computed with $(m - 1)$. This choice was made for two reasons. First, failure of combined cycle unit is more probable statistically, and second, the loading of steam units of Type 2 is limited due to environmental concerns, and so, its trip is not considered a worst case contingency.

As the RES production will increase, the number of committed synchronous units will decrease. Additionally, the response from each combined cycle unit will also be smaller, since the time until the frequency nadir will decrease due to lowered system inertia. Therefore, additional response is needed, and it can be achieved using PV facilities.

2.3. The Available Response of a PV Plant

The power of each photovoltaic cell depends on the solar irradiance levels and the cell's temperature. Other factors, such as the lack of coordination between cells resulting from partial shading, aging of cells, etc., are to be taken into account as well. A more detailed description of PV cell behavior according to the change in radiation and temperature may be found in [33], while a more practical implementation of reserve saving and participating in frequency response is described in [10]. A PV array is usually operated at a maximum power point (MPP) by controlling the output voltage of the cells using a DC/DC converter. A large number of maximum power point tracking (MPPT) methods [34,35] and strategies of arrays architecture [36] were developed, in order to achieve the best energy extraction.

The well-known and widely used MPPT methods are based on varying the applied voltage by DC/DC converter until it is determined at which point the produced power is maximum. In other words, the PV panel must be at the MPP point in order to determine it. For a deloaded operation, such methods do not work. In this case, the estimation of available power needs to rely on special methods. For example, it can be based on irradiance, on temperature measurements and preliminary calculations, as described in [10], or on dedicated reference inverters, as proposed in [37]. Based on the same principle of control with a DC/DC converter, the output power of a PV facility can be set below the maximum value in order to maintain a needed reserve and the capability to respond to a frequency decline. It is also important to calculate the needed response correctly, due to the cost implications of curtailing or reserving power. Curtailing power unnecessarily can result in the waste of clean energy and additional costs. On the other hand, reserving too little power can result in blackouts and other system failures, which can have even greater costs associated with them.

Figure 7 shows the principal structure of a large PV farm with frequency control capability. A control unit obtains the value of maximum power that can be generated from solar panels at the current irradiance and temperature levels and the amount of the reserve to be maintained according to the requirements of the system operator.

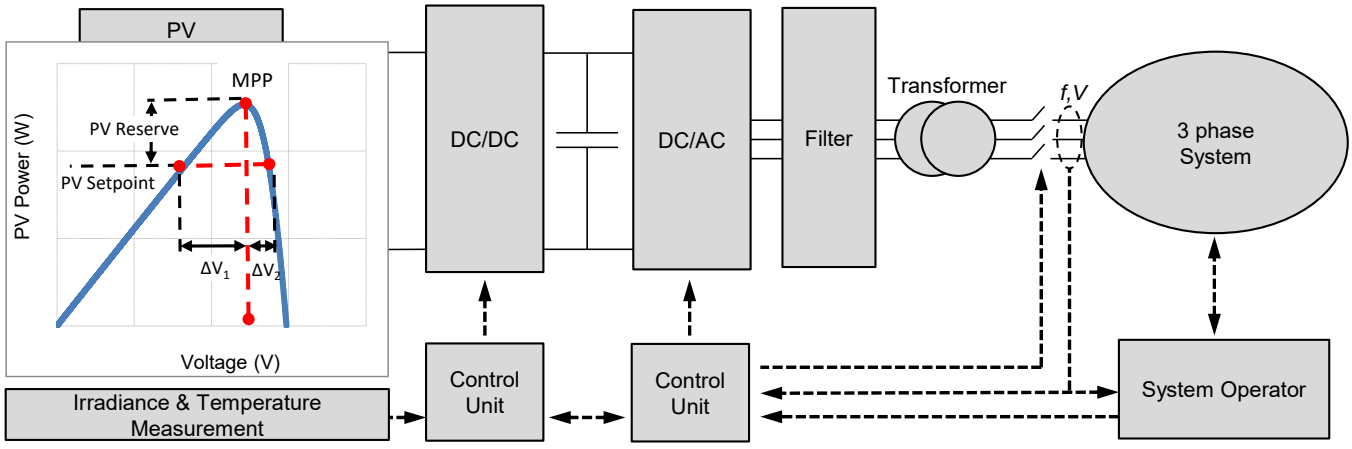

Figure 7. A principal scheme of PV facility with frequency-power control.

Depending on the requirements of the system operator, PV facilities of this type can provide different auxiliary services. Proportional frequency response (PFR) and step frequency response (SFR) from a PV plant were tested, with parameters based on [27] and appear in Figure 8.

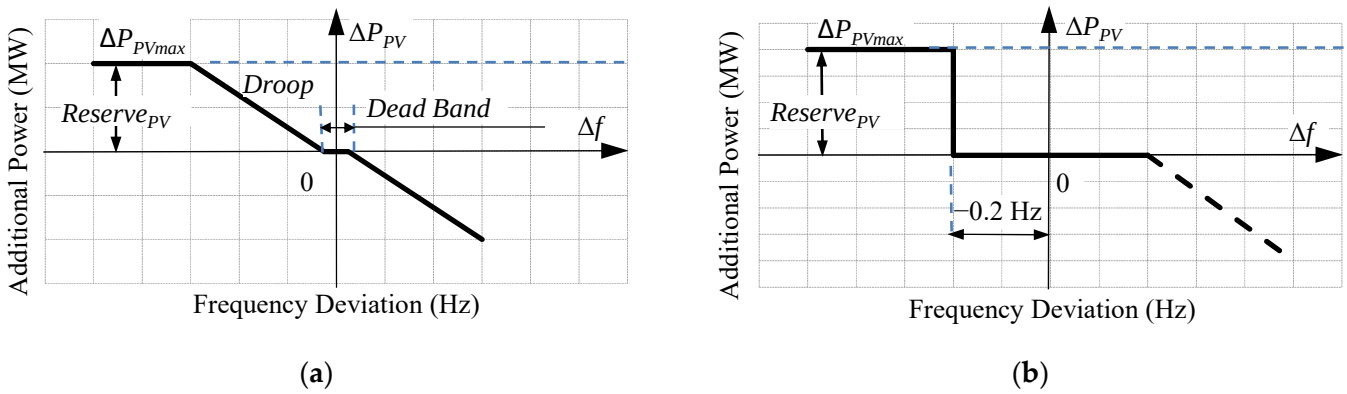

Figure 8. Two types of PV plant frequency response: (**a**) PFR; (**b**) SFR.

Due to the quick response time of converters [27–29], all the reserve that is kept in PV facilities may be used until the frequency reaches the minimum point. The required reserve from PV facilities ($Reserve_{PV}$) can be estimated as a supplement to the synchronous units' response:

$$Reserve_{PV} = \underbrace{\Delta P}_{\text{I}} - \underbrace{D * P_{LOAD} * \frac{\Delta f}{f_{nom}}}_{\text{II}} - \underbrace{n * RES_{SU2}}_{\text{III}} - \underbrace{(m-1)\alpha_{CC}\frac{\Delta f(J_{SYS} - J_{FO})8\pi^2 f_0}{\Delta P}}_{\text{IV}}. \quad (8)$$

The first part of (8) represents the initial power imbalance, or the size of the contingency. The second part represents the load relief, and the third and fourth parts estimate the synchronous units' fixed-size response and time-dependent response, respectively.

The proposed methodology to derive sufficient frequency response to prevent UFLS may be summarized in the following steps:

- Calculate *Load Relief* (4) for desired frequency deviation Δf;
- Estimate time until the frequency nadir t_{FN} (6) based on system inertia for given unit commitment;
- Determine available primary response of synchronous units $Response_{SG}$ (7);
- Supplement the system response by reserving PV power (8) to cover the size of contingency.

3. Results

The proposed energy-based method is general and developed equation for required PV reserve (8) can be implemented for every power system. So, the analysis of the Israeli system in this section was carried out to demonstrate the advantages of this method as a quick and effective tool to define range of response problem and also to assess how much supplemental response is required. Additionally, it was shown how this method helps to estimate profitability of different solutions for improving frequency stability.

Equation (8) was used to compute the necessary reserve from PV facilities in Israel for the next ten years. This was carried out for two different cases. First, we consider the case where, by 2030, 17% of Israel's annual electricity production based on RES. This is the renewable energy goal that the Israeli ministry of energy had set in 2018 [38]. The expected changes in the generation fleet were considered: replacing of production units, addition of pumped storage, and load-frequency sensitivity descent (see Appendix A for more information about Israeli grid). Second, we consider the case where, by 2030, 30% of Israel's annual electricity production based on RES, reflecting the latest goals set by the

Israeli ministry of energy in 2020 [39]. For all computations, we used linear extrapolation from true data collected in the Israeli power system in 2018.

3.1. Case 1: 17% Renewable Energy in Year 2030

As of today, Israel has coal-fired production units that, due to technological constraints, cannot be stopped for a short period of time and must remain connected to the system. Together with the cogeneration facilities, they provide must run power of about 2500 MW. In our calculation, when the *Residual Load* was lower than the must run power production, it was assumed that PV production was curtailed.

Only combined cycle units may by disconnected according to decline of the *Residual Load*. Their number m was calculated according to its minimum power P_{minCC}, in the iterative way:

$$m(1) = int\left[\frac{Residual\ Load - Must\ Run}{P_{minCC}}\right], \tag{9}$$

$$m(2) = int\left[\frac{(Residual\ Load + Reserve_{PV}) - Must\ Run}{P_{minCC}}\right].$$

The second iteration in (9) was considered because the $Reserve_{PV}$ power should be subtracted from RES production, so it must be generated by synchronous units.

Table 2 details the response from the synchronous units, load relief, and required reserve from PV facilities for 10 years, as it was calculated in Case 1, with 17% of RES by 2030.

Table 2. Required Reserve from PV Facilities, Case 1–17% RES.

Year	RES Energy	Min. Res. Load	Number of Units w/Response		SG Response	Load Relief		PV Reserve
	%	MW	SU–T2	CC	MW	%MW/%Hz	MW	MW
2021	7.2	4158	4	7	235	0.95	64	51
2022	8.3	3842	4	5	195	0.90	63	92
2023	9.4	3875	-	9	131	0.85	61	158
2024	10.5	3568	-	8	108	0.80	59	183
2025	11.6	3267	-	7	86	0.75	57	207
2026	12.6	3126	-	6	67	0.70	55	228
2027	13.7	2836	-	5	50	0.65	52	248
2028	14.8	2551	-	4	34	0.60	49	266
2029	15.9	2271	-	3	21	0.55	47	283
2030	17	1990	-	2	9	0.50	43	297

As seen in Table 2, the minimum residual load decreases with years, which is a result of PV production increasing faster than the system load. The number of combined cycle units that can remain connected decreases, and the sum of the responses of the synchronous units decreases according to the number of units and the decrease in the system inertia. According to the electricity system developing plan [38], coal-fired steam units with fast response will have been retired by 2023, affecting the must run power and synchronous response significantly. Starting in 2023, the must run power was set to 2040 MW. Additionally, the computations took into account two pumped storage facilities that will be added in 2023 and 2026, increasing the residual load accordingly.

It is important to recognize a decreasing trend in load-frequency sensitivity. The multiple factors, such as the load composition, the share of electric motors (induction and synchronous), and the types of the mechanical load that are operated by them affect

this characteristic. Loads connected to the system through converters (e.g., inverter air conditioner) are not affected by frequency change. Assuming that share of this types of loads will increase [31,40], the load-frequency sensitivity is expected to decrease, that was applied by reducing D from 0.95 to 0.5 over the years, as detailed in Table 2.

In the year 2030, the number of combined cycle units will have decreased to two, with response contribution from synchronous units of 9 MW only. Therefore, the response for arresting the frequency needs to be provided by the PV facilities increase to 297 MW.

To test the computation by (8), we conducted a dynamic simulation for 2021 (Figure 9). The frequency of the system following a 350 MW trip with response from the synchronous units only is marked in red. Indeed, response with solely synchronous units was insufficient and allowed the frequency to drop to 49.35 Hz, which is lower than the threshold 49.45 Hz was set.

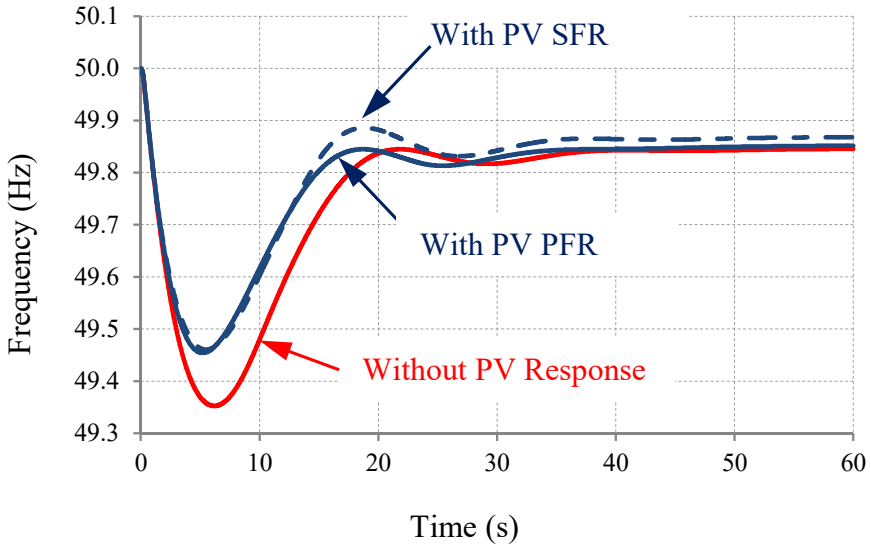

Figure 9. System frequency response to 350 MW generator trip, at minimum residual load point of the year 2021, Case 1.

In contrast, the system frequency with PV response is marked in blue. We tested both the PFR and the SFR characteristics that were described in the methods section. The PFR (solid blue line) was determined with a typical droop of 5% and 0 deadband. The nominal power of PV facilities with the PFR capability was set to 236 MW, which allowed to use the entire reserve, with respect to the 5% drop and defined frequency deviation of 0.55 Hz. This information is important to show that a relatively small part of the total installed PV capacity must have frequency-power control capability. In this case, it constitutes 11.4% of the total installed PV capacity in the system. The SFR (dashed blue line) was determined with a power surge within 500 ms after the frequency reaches 49.8 Hz. In both cases, the system response was satisfactory, and the frequency did not drop below 49.46 Hz.

We conducted a simulation for 2023 as well, including the response from the combined cycle units only, requiring a supplement of 158 MW from PV facilities (Figure 10). In the case of a serious lack of response from the synchronous units, the frequency dropped low, reaching about 49.05 Hz (red line). The addition of the response from the PV facilities resulted in a frequency above the set threshold. In the current simulation, the nominal power of PV facilities with a response capability of 718 MW was needed. It constituted 19.1% of the total installed PV capacity in the system. The PFR (solid blue line) arrested the frequency at 49.46 Hz. The SFR (dashed blue line) resulted in a slightly different minimum point, namely 49.51 Hz.

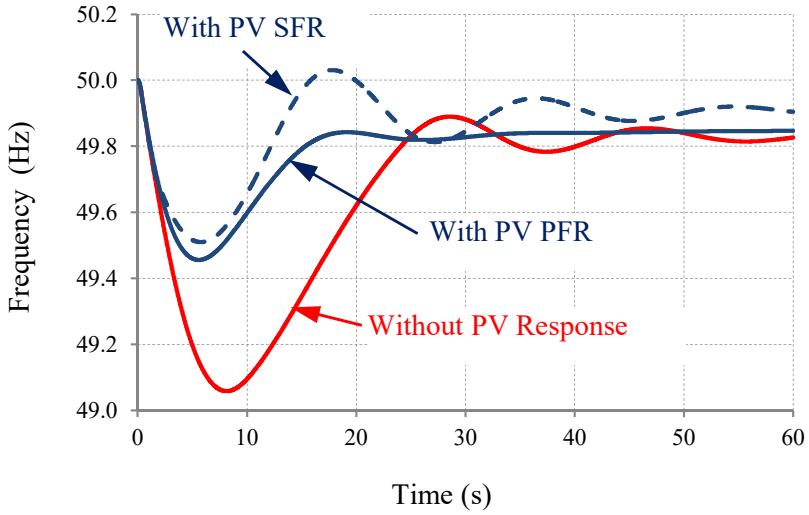

Figure 10. System frequency response to 350 MW generator trip, at minimum Residual Load point of the year 2030, Case 1.

These dynamic simulations, as response clustering study for synchronous units shown in Section 2, were carried out with the help of software developed in the Israel Electric Corporation (IECo), based on standard IEEE and WECC models. However, adjustments were made to these models for specific units, in order to achieve an optimal match of the model to the actual performance. Details of the software and of the models are not provided here due to confidential requirements; at the same time, there is no necessity either. Dynamic simulations were performed only in order to determine the result of the calculation carried out by (8) and to prove its quality. Anyone interested in using the proposed method and verifying the calculations with dynamic simulation can run the simulation with their preferred tool to obtain reliable results.

The required reserve of PV facilities in every year as appear in Table 2 refers to the minimum Residual Load. In practice, the problem persists for a range of power. Figure 11a details the Residual Load throughout 2030, marking Range of Response Problem. The response needed from the PV facilities in this range was again computed with (8), and the appropriate number of hours is detailed in Figure 11b.

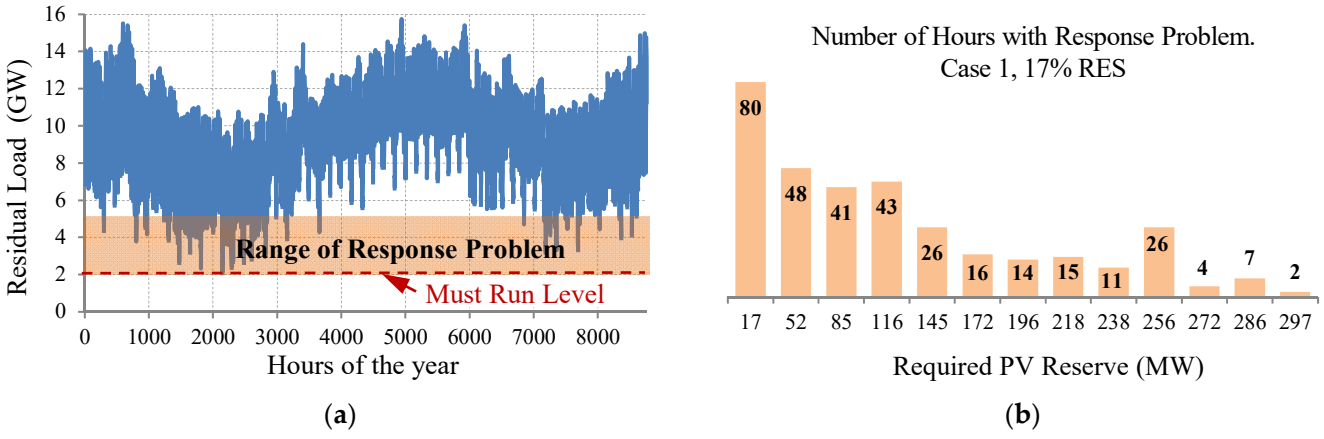

Figure 11. (**a**) Residual Load through the year 2030; (**b**) distribution of necessary PV Reserve in the Range of the Response Problem, Case 1.

In Case 1, for most of the hours in 2030, the Israeli power system can provide a response with synchronous units solely. At least 15 combined cycle units are needed to prevent UFLS due to a 350 MW generator trip. Residual Load of 5400 MW is needed to

operate them. The value of 5400 MW defines the border level, below which the system is incapable of withstanding the contingency without load shedding. Only for 475 h (about 5.4% of the hours of the year) the Residual Load was below 5400 MW, and there was need for reserve power in PV facilities to complete the sufficient response. As expected, this situation occurred mostly in off-peak seasons and weekends, when the system demand was relatively low.

3.2. Case 2: 30% Renewable Energy in Year 2030

In Case 2, PV production was significantly increased to reach the 30% goal. The initial computation determined that the required capacity of PV facilities in 2030 will be 15,200 MW. A detailed analysis revealed significant curtailment of PV energy during hours when the residual load was lower than must run level. This curtailment reduced the RES production from 30% of the annual energy to 27.6%. Therefore, more PV capacity was needed to compensate this curtailment. Updated PV capacity was set to 16,200 MW. A similar adjustment was made in the years 2026–2029.

All the assumptions regarding the composition of units and the load-frequency sensitivity that were detailed in Case 1 remained unchanged. The results of the computation with (8) are detailed in Table 3.

Table 3. Required Reserve from PV Facilities, Case 2–30% RES.

Year	RES Energy	Min. Res. Load	Number of Units w/Response		SG Response	Load Relief		PV Reserve
	%	MW	SU–T2	CC	MW	%MW/%Hz	MW	MW
2021	7.2	4158	4	7	235	0.95	64	51
2022	9.7	2747	4	1	140	0.90	63	147
2023	12.3	2230	-	2	9	0.85	61	280
2024	14.8	1353	-	1	0	0.80	59	291
2025	17.3	480	-	1	0	0.75	57	293
2026	19.9	−296	-	1	0	0.70	55	295
2027	22.4	−1247	-	1	0	0.65	52	298
2028	24.9	−2193	-	1	0	0.60	49	301
2029	27.5	−3298	-	1	0	0.55	47	303
2030	30	−4398	-	1	0	0.50	43	307

In Case 2, the residual load decreased across the years very fast, and in 2024, there were already hours when only must run units were connected to the system. From this year, the response required from PV facilities increased slightly due to attenuation in load-frequency sensitivity. By 2024, the number of combined cycle units will have decreased to 1, which nullifies the response contribution from synchronous units. Therefore, all the response for arresting the frequency needs to be provided by the PV facilities. In 2030, the reserve needed from PV facilities was 307 MW. However, the most important, that number of hours with response problem increased dramatically. Figure 12a displays the change in residual load throughout 2030, and the range of response problem, that remained the same as in Case 1. In 30% RES scenario within 2384 h (27.2% of the year), the residual load was below 5400 MW, and the response from PV facilities was required, as shown in Figure 12b. Within 938 h, the residual load was below the must run level, resulting in curtailment of PV-produced energy.

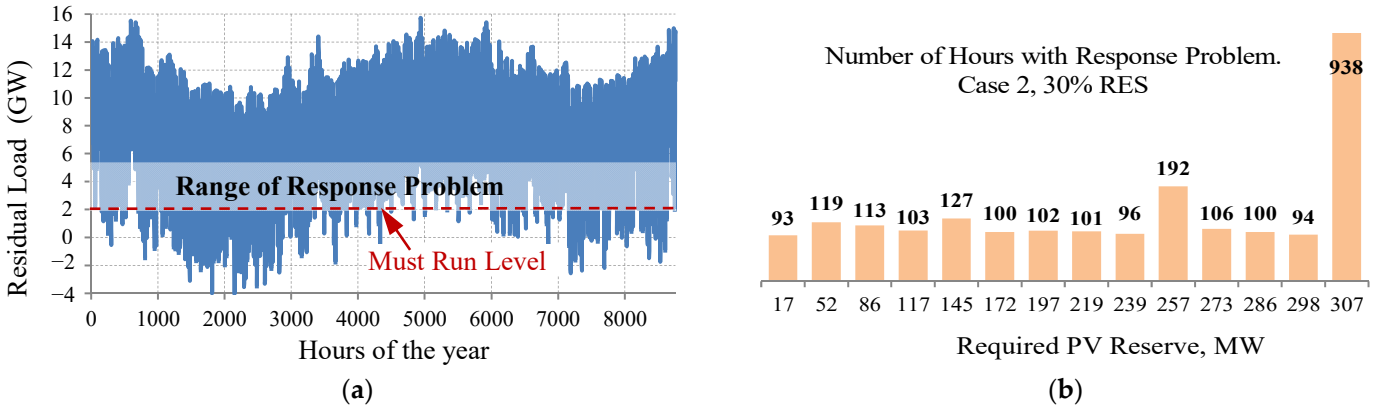

Figure 12. (**a**) Residual Load through the year 2030; (**b**) distribution of necessary PV reserve in the Range of the Response Problem, Case 2.

3.3. Incremental Cost Analysis

It was interesting to compare the incremental costs of several solutions of the response problem:

(1) Saving the reserve in the PV facilities;
(2) Keeping the number of combined cycle units that allow sufficient synchronous response. This option would involve further curtailment of power production from renewable energy sources;
(3) Adding open cycle gas turbines. While gas turbines are less efficient than combined cycle units, their minimum power is lower, allowing significantly reduce curtailment of PV production;
(4) Installing a battery energy storage system (BESS) for frequency control [9].

In the following computations, the yearly increase in the two components of the electricity production cost was taken into consideration: CAPEX (Capital Expense) and OPEX (Operating Expenses). For the first three solutions above, no change was assumed in CAPEX and in the constant part of OPEX, since they use existing facilities. The main difference between the costs of the first three solutions was due to changes in the variable part of OPEX, i.e., fuel consumption. For the fourth solution, BESS, there was no fuel cost, but it needs to be installed. The CAPEX cost and the constant OPEX cost were evaluated and spread over the life expectancy of the facility, resulting in a yearly cost. Table 4 summarizes the data that were used to compute the annual cost of BESS for 2030 using an intermediate forecast for the utility-scale lithium-ion batteries in [41].

Table 4. Annual cost calculation for 0.75 h BESS.

Parameter	Value	Units
Specific capital cost of power components	150	$/kW
Specific capital cost of energy components	170	$/kWh
Energy storage capacity (hours of nominal output)	0.75	hours
Annual battery system O&M cost (as percent of CAPEX)	2.5	%
Project life	15	years
Interest Rate	3.5	%
Overall annual cost	31,031	$/kW/Year

Table 5 summarizes the incremental costs of operating the system in 2030 while providing sufficient response to 350 MW unit trip, preventing load shedding, for each of the four solutions.

Table 5. Incremental Cost of Sufficient Frequency Response for year 2030.

Solution	Case 1 17% RES	Case 2 30% RES
1. Reserve power in PV facilities		
Expended energy, GWh	53.9	282.0
Incremental cost, M $	3.34	17.46
2. with Combined Cycle		
Expended energy, GWh	486.2	5922.5
Incremental cost, M $	20.38	248.23
3. with Gas Turbine (open cycle)		
Expended energy, GWh	101.3	1233.9
Incremental cost, M $	7.44	90.62
4. BESS for frequency regulation		
BESS Power, MW	307	307
Incremental cost, M $	9.53	9.53

The additional fuel cost for the combined cycle and gas turbine solutions was computed based on the average production cost, in accordance with the type of the unit. Due to fluctuations in the costs of fossil fuels and the difficulty of predicting trends until 2030, we used the current cost of fossil fuels. According to [42], the average cost of electricity production using combined cycle units was 4.16 US cents per kWh, while the production cost with gas turbines was 7.35 US cents per kWh. The costs in Israeli New Shekels (ILS) were exchanged to United States Dollars (USD) according to the mean exchange rate of 2019, 1 USD = 3.5645 ILS [43]. This conversion rate was chosen to match the batteries costs, which are based on 2019 USD [41].

A conservative approach was taken when considering the solution based on the reserve from PV. There are two costs involved in the cost of energy that could have been produced by a PV facility but was instead reserved for the purposes of frequency response. It consists of the production cost for the PV producer and the cost of producing the same energy with a combined cycle unit instead. Hours when the residual load was below the must run level were not included, since this energy could not have been used then. According to a forecast of the American Department of Energy [44], the cost of energy produced by utility-scale PV is expected to decrease to 2 US cents per kWh in 2030. The computations of energy costs in PV facilities were performed using these data. Annual amounts of expended energy were computed according to the distribution of power and hours within the response problem range, as shown in Figures 11 and 12, for two tested cases.

As seen in Table 5, for Case 1, the lowest incremental cost was found for the solution of keeping the reserve in the PV facilities. In the case with a goal of 17% of electricity production by RES, the hours with a reserve problem were few and concentrated in days with low load demand (weekends and off-peak seasons). In Case 2, with a goal of 30% of electricity production by RES, the number of days and hours with reserve problem increased significantly, making the option of keeping the reserve in the PV facilities less profitable. Instead, the BESS for frequency control was the most profitable among the suggested options. Solutions that relied on preserving response capabilities using synchronous units not only proved to be more expensive, but also to make inappropriate use of renewable energy sources, and to exacerbate air pollution.

More precisely, installing a BESS could provide additional benefits to operating the electricity system. Therefore, the annual cost for the BESS could be offset by these benefits. On the other hand, more intensive use of batteries would increase the number charge–discharge cycles, shortening the lifetime expectancy of the BESS facility.

The main conclusion from the economical assessment is that saving the reserve in PV facilities could be a preferable option for low to medium-scale renewable energy

production. However, with larger-scale renewable energy production (e.g., 30%), installing a BESS facility was found to be the most profitable solution. Equation (8), which was developed in the current study, is an efficient and quick tool for evaluating the profitability of various solutions.

4. Discussion

Appropriate frequency response is an issue of great importance in a power system and would appear to pose significant limitations on the extensive integration of renewable generation. Prior studies proposed detailed investigations for certain scenarios of RES penetration by using dynamic simulations that rely on the properties of individual systems. While simulations are valuable, they require dedicated software, they are time-consuming, their results are relevant mostly to the specific system under discussion, they cover a limited time range, and any change in the model parameters requires repeating the entire simulation process.

In this paper, we proposed an alternative energy-based approach, which was checked by comparison with the results of the standard method based dynamic simulations. Our approach estimates the amount of the additional fast power injection to prevent UFLS. The new equation was proposed, connecting:

- size of contingency;
- inertia of system;
- load behavior;
- available response of synchronous generating units.

The range of response problem was defined by minimal number of generation units, required to produce a sufficient response to prevent load shedding. When the residual load was below the defined level, the amount of PV reserve was required.

Synchronous generation units were clustered into three, according to their ability to respond in low-inertia state. In every power system, the same process of clustering for synchronous generation units may be applied. One cluster of the units was defined to have zero-response; their contribution to the system response was inertia only. Another cluster had a fast response, such that in the relevant time window, it produced an almost uniform response. This cluster's contribution to the system response was inertia and power injection of a fixed size. Finally, last cluster was mostly defined by its linear relationship between the time of the frequency nadir and their response capability. Third cluster's contribution to the system response was inertia and time-dependent power injection. Separation of units into clusters allows to assess the potential synchronous response, which provides information about its deficiency in defined system state. The amount of supplementary reserve from PV facilities or other invertors based sources may be found by the developed Equation (8).

In this study, the additional fast response was chosen to be provided by PV facilities. However, other fast response sources may also be used, such as batteries or demand side response, the latter presumably requiring some adjustments. Future work is needed to establish the use of the equation in other applications.

We used the proposed method to compute how much response is needed from PV facilities in the Israeli system for the next 10 years (this study was carried out as part of the first author's PhD degree and presents only the professional opinion of the authors). We conducted the computation separately for different percentages of renewable energy (17% and 30% in year 2030) according to the renewable energy goals set by the state. Along the way, many more scenarios were tested with different percentages of renewable energy. This is the strength of the proposed method that a result is obtained immediately (provided that all input data are already prepared). It was taken into consideration changes in the generation fleet, integration of pumped storage facilities, and decrease in the load sensitivity to changes in frequency. Additionally, we defined the Range of Response Problem and calculated the yearly distribution of hours according to the required PV response. This calculation was also conducted using the proposed equation. These results were used as input for computing the profitability of different solutions to the frequency response

problem. Interestingly, when the renewable energy goal was 17%, the most profitable solution was a response from PV facilities, whereas when the renewable energy goal was raised to 30%, the most profitable solution was installing BESS for frequency control.

It is important to note that there are many regions in the world with strong and stable solar radiation for most of the year with variability during the hours of the day that are known in advance. In this case, it is easy to estimate the available power for PV facility and to maintain the required reserve to achieve the desired system response. We also wish to emphasize again that using PV capabilities for frequency stability does not require building additional facilities, as in the case of BESS. Moreover, in all scenarios, PV solution is cheaper and more environmentally friendly than using fossil units for the same purpose.

According to our results, as early as 2021, the response of synchronous units needed to be supplemented by reserve in PV facilities. This need will increase constantly as PV production increases over the next years.

In this study, we kept the size of the contingency constant to keep the trends of interest transparent. For the 350 MW contingency in all tested scenarios, the resulting ROCOF was within the allowed limits, due to relatively large must run level. In practice, the size of the contingency must be adjusted as larger units enter the fleet or in consideration of other possible contingencies. Larger units or smaller must run level might result in a ROCOF beyond the allowed limits, which can put the systems security at risk [45]. This will require other solution, either through limiting the power of production units in order to reduce the size of possible contingency, or adding inertia to the system using synchronous condensers [12,46], or inverters with properties of synchronous machines [47].

This method is valuable for investigating frequency stability issues and for allowing a broad view for future system planning. Using the research results will help speed up this procedure and allow exploring more options in less time. This, in turn, makes easier the integration of PV facilities in the power system, maintaining sufficient frequency response and, potentially, even improving the reliability of the electricity supply to consumers. In fact, the proposed energy-based method is general and system-independent; the analysis of Israeli system was carried out for demonstration purpose only.

Another direct effect of RES on frequency stability of the power system is due to variable and unpredictable nature of solar and wind energy. In order to overcome this problem, adjusted levels of regulating reserve are needed, which must be dynamic, variable during the day and according to the fraction of renewable generation [48].

While one of the strengths of the proposed method is its generality and simplicity, it should be noted that we posited some assumptions and approximations to achieve this. For example, the swing equation and electrical load power representation by linear dependence on frequency do not consider inter-generator swings, which may by detailed in simulation. These assumptions and approximations impact the precision of calculations with this method, but, in our case study, any imprecision caused by them proved to be acceptable. Furthermore, in cases of interest, detailed simulation could be conducted to validate the results from the calculations with proposed equation.

When researching RES penetration impacts, of key interest are both the frequency and the voltage stability. The focus of this study was the effect of PV generation on frequency dynamics. However, voltage stability issues caused by nonsynchronous generation are not within the scope of this study. In future work, coordination between voltage and frequency stability must be investigated to be able to appropriately plan future strategies of PV integration.

Author Contributions: Conceptualization, O.P.; methodology, O.P.; validation, O.P.; formal analysis, O.P.; investigation, O.P.; data curation, O.P.; writing—original draft preparation, O.P.; writing—review and editing, O.P. and D.S.; visualization, O.P.; supervision, D.S. All authors have read and agreed to the published version of the manuscript.

Funding: This research received no external funding.

Data Availability Statement: The data that support the findings of this study are available from the corresponding author upon reasonable request.

Conflicts of Interest: The authors declare no conflict of interest.

Appendix A

A principle scheme of power system in Israel presented in Figure A1, with reference to primary energy resources [49]. As per the 2018 data, the installed capacity was about 17,600 MW, including renewable energy facilities of 1000 MW, based mainly on PV, and two solar thermal power plants. Currently, thousands of megawatts of PV are added to the system, as part of the global effort to decarbonize power sector and reduce global warming.

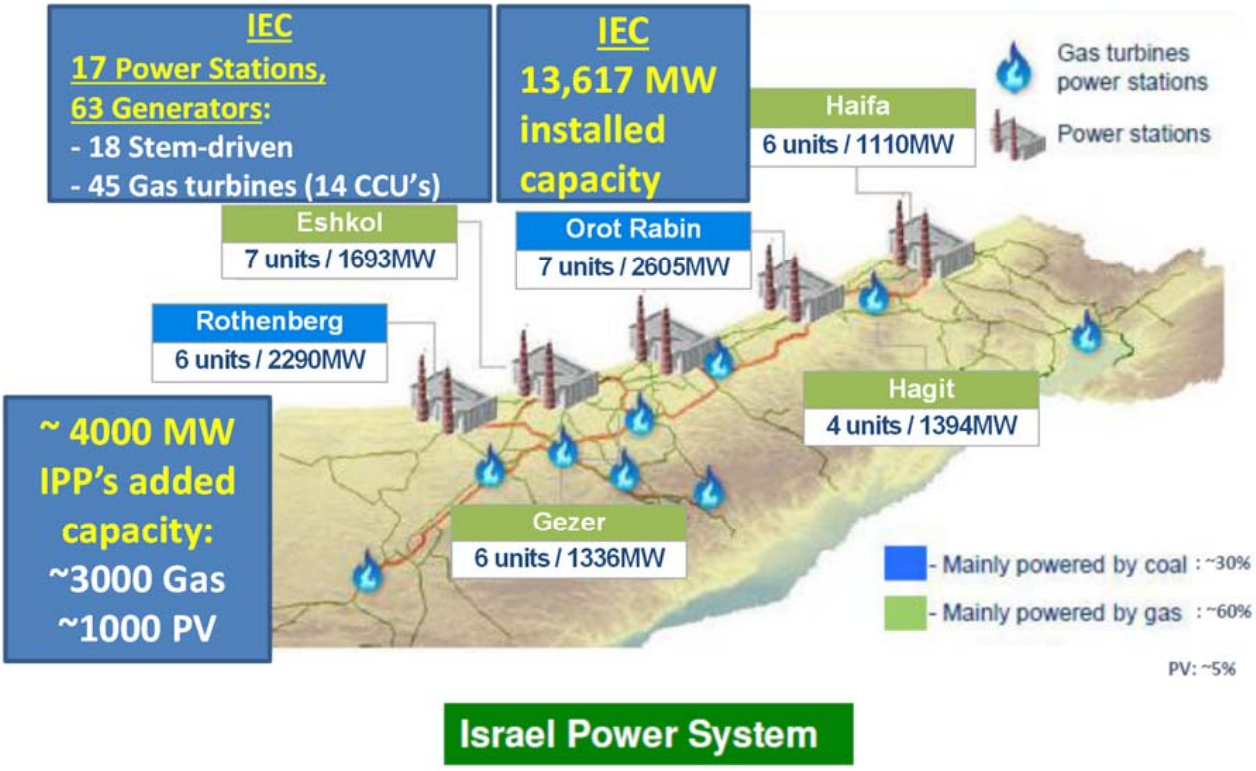

Figure A1. A principal scheme of Israel Power System.

References

1. Anderson, P.; Fouad, A. *Power System Control and Stability*; The Iowa State University Press: Ames, IA, USA, 1982.
2. Kundur, P. *Power System Stability and Control*; McGraw Hill LNC.: New York, NY, USA, 1994.
3. O'Sullivan, J.; Rogers, A.; Flynn, D.; Smith, P.; Mullane, A.; O'Malley, M. Studying the Maximum Instantaneous Non-Synchronous Generation in an Island System—Frequency Stability Challenges in Ireland. *IEEE Trans. Power Syst.* **2014**, *29*, 2943–2951. [CrossRef]
4. Wang, Y.; Delille, G.; Bayem, H.; Guillaud, X.; Francois, B. High Wind Power Penetration in Isolated Power Systems—Assessment of Wind Inertial and Primary Frequency Responses. *IEEE Trans. Power Syst.* **2013**, *28*, 2412–2420. [CrossRef]
5. Miller, N.W.; Shao, M.; Venkataraman, S.; Loutan, C.; Rothleder, M. Frequency response of California and WECC under high wind and solar conditions. In Proceedings of the 2012 IEEE Power and Energy Society General Meeting, San Diego, CA, USA, 22–26 July 2012; pp. 1–8.
6. Miller, N.W.; Shao, M.; D'aquila, R.; Pajic, S.; Clark, K. Frequency Response of the US Eastern Interconnection Under Conditions of High Wind and Solar Generation. In Proceedings of the 2015 Seventh Annual IEEE Green Technologies Conference, New Orleans, LA, USA, 15–17 April 2015; pp. 21–28.
7. Wang, Y.; Silva, V.; Lopez-Botet-Zulueta, M. Impact of high penetration of variable renewable generation on frequency dynamics in the continental Europe interconnected system. *IET Renew. Power Gener.* **2016**, *10*, 10–16. [CrossRef]
8. Vasconcelos, H.; Moreira, C.; Madureira, A.; Lopes, J.P.; Miranda, V. Advanced Control Solutions for Operating Isolated Power Systems: Examining the Portuguese islands. *IEEE Electrif. Mag.* **2015**, *3*, 25–35. [CrossRef]

9. Ben Yosef, G.; Navon, A.; Poliak, O.; Etzion, N.; Gal, N.; Belikov, J.; Levron, Y. Frequency stability of the Israeli power grid with high penetration of renewable sources and energy storage systems. *Energy Rep.* **2021**, *7*, 6148–6161. [CrossRef]
10. Hoke, A.; Muljadi, E.; Maksimovic, D. Real-time photovoltaic plant maximum power point estimation for use in grid frequency stabilization. In Proceedings of the 2015 IEEE 16th Workshop on Control and Modeling for Power Electronics (COMPEL), Vancouver, BC, Canada, 12–15 July 2015; pp. 1–7.
11. Ahmadyar, A.S.; Riaz, S.; Verbic, G.; Chapman, A.; Hill, D.J. A Framework for Assessing Renewable Integration Limits with Respect to Frequency Performance. *IEEE Trans. Power Syst.* **2017**, *33*, 4444–4453. [CrossRef]
12. Gu, H.; Yan, R.; Saha, T.K. Minimum Synchronous Inertia Requirement of Renewable Power Systems. *IEEE Trans. Power Syst.* **2017**, *33*, 1533–1543. [CrossRef]
13. Liu, Y.; You, S.; Tan, J.; Zhang, Y.; Liu, Y. Frequency Response Assessment and Enhancement of the U.S. Power Grids Toward Extra-High Photovoltaic Generation Penetrations—Anndustry Perspective. *IEEE Trans. Power Syst.* **2018**, *33*, 3438–3449. [CrossRef]
14. Trovato, V.; Bialecki, A.; Dallagi, A. Unit Commitment with Inertia-Dependent and Multispeed Allocation of Frequency Response Services. *IEEE Trans. Power Syst.* **2018**, *34*, 1537–1548. [CrossRef]
15. Zhao, X.; Wei, H.N.; Qi, J.; Li, P.; Bai, X. Frequency Stability Constrained Optimal Power Flow Incorporating Differential Algebraic Equations of Governor Dynamics. *IEEE Trans. Power Syst.* **2020**, *36*, 1666–1676. [CrossRef]
16. Shen, J.; Li, W.; Liu, L.; Jin, C.; Wen, K.; Wang, X. Frequency Response Model and Its Closed-Form Solution of Two-Machine Equivalent Power System. *IEEE Trans. Power Syst.* **2021**, *36*, 2162–2173. [CrossRef]
17. Atkinson, J.; Albayati, I. Impact of the Generation System Parameters on the Frequency Response of the Power System: A UK Grid Case Study. *Electricity* **2021**, *2*, 143–157. [CrossRef]
18. Liao, S.; Xu, J.; Sun, Y.; Gao, W.; Xu, L.; Huang, L.; Li, X.; Gu, J.; Dong, J. WAMS-based frequency regulation strategy for photovoltaic system in isolated power systems. In Proceedings of the 2015 IEEE Power Energy Society General Meeting, Denver, CO, USA, 26–30 July 2015; pp. 1–5.
19. Liao, S.; Xu, J.; Sun, Y.; Bao, Y.; Tang, B. Wide-area measurement system-based online calculation method of PV systems de-loaded margin for frequency regulation in isolated power systems. *IET Renew. Power Gener.* **2017**, *12*, 335–341. [CrossRef]
20. Lim, S.; Kim, T.; Yoon, K.; Choi, D.; Park, J.-W. A Study on Frequency Stability and Primary Frequency Response of the Korean Electric Power System Considering the High Penetration of Wind Power. *Energies* **2022**, *15*, 1784. [CrossRef]
21. FERC. *Essential Reliability Services and the Evolving Bulk-Power System-Primary Frequency Response*; FERC: Washington, DC, USA, 2018.
22. ENTSO-E. Requirements for Generators. *European Association for the Cooperation of Transmission System Operators (TSOs) for Electricity.* 2016. Available online: https://www.entsoe.eu/network_codes/rfg/ (accessed on 3 July 2021).
23. Cabrera-Tobar, A.; Bullich-Massagué, E.; Aragüés-Peñalba, M.; Gomis-Bellmunt, O. Review of advanced grid requirements for the integration of large scale photovoltaic power plants in the transmission system. *Renew. Sustain. Energy Rev.* **2016**, *62*, 971–987. [CrossRef]
24. EirGrid. *EirGrid Grid Code*; Version 9; EirGrid: Dublin, Ireland, 2020.
25. National Grid Electricity System Operator (UK). *Grid Code*; Issue 6, Revision 3; National Grid ESO: London, UK, 2021.
26. IECo. Requirements for Connecting Photovoltaic Facilities to a High Voltage System. Electricity Authority (Israel). 2018. Available online: https://www.gov.il/BlobFolder/policy/55011/he/Files_Hachlatot_55011_1304_nisp_yod_7.pdf (accessed on 3 July 2021).
27. Gevorgian, V.; O'Neill, B. *Advanced Grid-Friendly Controls Demonstration Project for Utility-Scale PV Power Plants*; Report No.: NREL/TP-5D00-65368; National Renewable Energy Lab. (NREL): Golden, CO, USA, 2016. Available online: https://www.osti.gov/biblio/1236761 (accessed on 14 June 2021).
28. Loutan, C.; Klauer, P.; Chowdhury, S.; Hall, S.; Morjaria, M.; Chadliev, V.; Milam, N.; Milan, C.; Gevorgian, V. Demonstration of Essential Reliability Services by a 300-MW Solar Photovoltaic Power Plant. 2017. Available online: https://www.osti.gov/biblio/1349211 (accessed on 29 June 2021).
29. Machlev, R.; Batushansky, Z.; Soni, S.; Chadliev, V.; Belikov, J.; Levron, Y. Verification of Utility-Scale Solar Photovoltaic Plant Models for Dynamic Studies of Transmission Networks. *Energies* **2020**, *13*, 3191. [CrossRef]
30. Tielens, P.; Henneaux, P.; Cole, S. Penetration of renewables and reduction of synchronous inertia in the European power system–Analysis and solutions. *ASSET Proj.* **2018**, *8*, 1–72.
31. AEMO. Renewable Integration Study Stage 1, Appendix B: Frequency Control. *Australian Energy Market Operator.* 2020. Available online: https://www.aemo.com.au/energy-systems/Major-publications/Renewable-Integration-Study-RIS (accessed on 30 June 2021).
32. Matevosyan, J.; Sharma, S.; Huang, S.H.; Woodfin, D.; Ragsdale, K.; Moorty, S.; Wattles, P.; Li, W. Proposed future Ancillary Services in Electric Reliability Council of Texas. In Proceedings of the 2015 IEEE Eindhoven PowerTech, Eindhoven, The Netherlands, 29 June–2 July 2015; pp. 1–6.
33. Wenham, S.R.; Green, M.A.; Watt, M.E.; Corkish, R. *Applied Photovoltaics*, 2nd ed.; Earthscan: Oxford, UK, 2007.
34. Esram, T.; Chapman, P.L. Comparison of Photovoltaic Array Maximum Power Point Tracking Techniques. *IEEE Trans. Energy Convers.* **2007**, *22*, 439–449. [CrossRef]
35. Levron, Y.; Shmilovitz, D. Maximum Power Point Tracking Employing Sliding Mode Control. *IEEE Trans. Circuits Syst. I Regul. Pap.* **2013**, *60*, 724–732. [CrossRef]

36. Abramovitz, A.; Shmilovitz, D. Short Survey of Architectures of Photovoltaic Arrays for Solar Power Generation Systems. *Energies* **2021**, *14*, 4917. [CrossRef]
37. Gevorgian, V. *Highly Accurate Method for Real-Time Active Power Reserve Estimation for Utility-Scale Photovoltaic Power Plants*; Report No.: NREL/TP-5D00-73207; National Renewable Energy Lab. (NREL): Golden, CO, USA, 2019. Available online: https://www.osti.gov/biblio/1505550 (accessed on 14 June 2021).
38. Electricity Authority Israel. Roadmap for the Development of the Production Segment in the Electricity 2018–2030. Ministry of Energy. 2018. Available online: https://www.gov.il/he/departments/general/mapat_derech (accessed on 7 June 2021).
39. Electricity Authority Israel. Draft for Public Reference-Increasing the Targets for Electricity Generation with Renewables for 2030. Ministry of Energy. 2020. Available online: https://www.gov.il/he/departments/publications/Call_for_bids/shim_2030yaad (accessed on 15 June 2021).
40. NERC. *Fast Frequency Response Concepts and Bulk Power System Reliability Needs*; NERC: Atlanta, GA, USA, 2020.
41. Cole, W.; Frazier, A. *Cost Projections for Utility-Scale Battery Storage: 2020 Update*; Report No.: NREL/TP-6A20-75385; National Renewable Energy Lab. (NREL): Golden, CO, USA, 2020. Available online: https://www.osti.gov/biblio/1665769 (accessed on 14 June 2021).
42. Electricity Authority Israel, IECo. System Operator Data Production and Consumption Chapter. 2020. Available online: https://www.gov.il/he/departments/general/hovatdivuahnetunim (accessed on 8 September 2021).
43. Bank of Israel. Average Exchange Rates. 2020. Available online: https://www.boi.org.il/he/Markets/ForeignCurrencyMarket (accessed on 16 June 2021).
44. EERE. Goals ofhe Solar Energy Technologies Office. Energy.Gov. 2021. Available online: https://www.energy.gov/eere/solar/goals-solar-energy-technologies-office (accessed on 15 June 2021).
45. Yan, R.; Masood, N.A.; Kumar Saha, T.; Bai, F.; Gu, H. The Anatomy ofhe 2016 South Australia Blackout: A Catastrophic Event in a High Renewable Network. *IEEE Trans. Power Syst.* **2018**, *33*, 5374–5388. [CrossRef]
46. Payerl, C. Synchronous Condensers Rediscovered—A New Way to Strengthen Grids. Modern Power Systems. 2021. Available online: https://content.yudu.com/web/442ay/0A444rp/MPS0521-Pros/html/index.html?page=12&origin=reader (accessed on 3 July 2021).
47. Zhong, Q.-C.; Weiss, G. Synchronverters: Inverters that mimic synchronous generators. *IEEE Trans. Ind. Electron.* **2011**, *58*, 1259–1267. [CrossRef]
48. Ela, E.; Milligan, M.; Kirby, B. *Operating Reserves and Variable Generation*; Report, No.: NREL/TP-5500-51978; National Renewable Energy Lab. (NREL): Golden, CO, USA, 2011. Available online: https://www.osti.gov/biblio/1023095 (accessed on 14 June 2021).
49. IEC. 2018_National-Power-System_Israel. 2018. Available online: https://www.cigre.org/userfiles/files/Community/NC/2018_National-power-system_Israel.pdf (accessed on 21 March 2023).